



HAL
open science

Covalent bonds in α -SnF₂ monitored by J-couplings in solid-state NMR spectra

Thomas Braeuniger, Stefan Ghedia, Martin Jansen

► **To cite this version:**

Thomas Braeuniger, Stefan Ghedia, Martin Jansen. Covalent bonds in α -SnF₂ monitored by J-couplings in solid-state NMR spectra. *Journal of Inorganic and General Chemistry / Zeitschrift für anorganische und allgemeine Chemie*, 2010, 636 (13-14), pp.2399. 10.1002/zaac.201000176 . hal-00567268

HAL Id: hal-00567268

<https://hal.science/hal-00567268>

Submitted on 20 Feb 2011

HAL is a multi-disciplinary open access archive for the deposit and dissemination of scientific research documents, whether they are published or not. The documents may come from teaching and research institutions in France or abroad, or from public or private research centers.

L'archive ouverte pluridisciplinaire **HAL**, est destinée au dépôt et à la diffusion de documents scientifiques de niveau recherche, publiés ou non, émanant des établissements d'enseignement et de recherche français ou étrangers, des laboratoires publics ou privés.



Covalent bonds in α -SnF₂ monitored by *J*-couplings in solid-state NMR spectra

Journal:	<i>Zeitschrift für Anorganische und Allgemeine Chemie</i>
Manuscript ID:	zaac.201000176.R1
Wiley - Manuscript type:	Article
Date Submitted by the Author:	25-Jun-2010
Complete List of Authors:	Braeuniger, Thomas; MPI fuer Festkoerperforschung, Stuttgart, Abteilung Jansen, Chemie III Ghedia, Stefan; MPI fuer Festkoerperforschung, Abt. Jansen, Chemie III Jansen, Martin; MPI fuer Festkoerperforschung, Chemie III
Keywords:	19F-NMR, 119Sn-NMR, J-couplings, heteronuclear spin decoupling, alpha-SnF2



1
2
3
4
5
6
7
8
9
10
11
12
13
14
15
16
17
18
19
20
21
22
23
24
25
26
27
28
29
30
31
32
33
34
35
36
37
38
39
40
41
42
43
44
45
46
47
48
49
50
51
52
53
54
55
56
57
58
59
60

Covalent bonds in α -SnF₂ monitored by
J-couplings in solid-state NMR spectra

Thomas Bräuniger*, S. Ghedia, M. Jansen

June 25, 2010

Max-Planck-Institute of Solid-State Research,
Heisenbergstr. 1, 70569 Stuttgart, Germany

* Corresponding author. Fax: +49 711 689 1502.

E-mail address:

T.Braeuniger@fkf.mpg.de (T. Bräuniger).

Abstract

The stable ambient-temperature phase of tin(II) fluoride, α -SnF₂, has been studied by ¹⁹F and ¹¹⁹Sn magic-angle spinning (MAS) NMR spectroscopy. A large chemical shift anisotropy (CSA) is observed in the spectra of both nuclides, which is indicative of the presence of stereochemically active lone electron pair on Sn. Symmetric satellite lines with low intensity have been detected in the ¹¹⁹Sn MAS spectra acquired under ¹⁹F decoupling, and are assigned to indirect *J*-couplings between the magnetically active Sn isotopes. The detection of *J*-couplings is evidence for the existence of genuine covalent bonds in α -SnF₂, a fact which has been deduced before from X-ray crystallography, which revealed the presence of Sn–F distances smaller than the sum of the respective ionic radii.

Keywords

¹⁹F-NMR; ¹¹⁹Sn-NMR; J-couplings; heteronuclear spin decoupling; α -SnF₂

1 Introduction

Tin(II) fluoride, SnF₂, is known to crystallise as monoclinic phase (α -SnF₂) at ambient conditions [1, 2]. At elevated temperatures an orthorhombic phase (β -SnF₂) and a tetragonal phase (γ -SnF₂) also occur [3], which convert back to α -SnF₂ at standard conditions. The structure of α -SnF₂ is pictured in Fig. 1. It is constructed from an asymmetric unit that contains two tin and four fluorines [1]. Both these elements may be observed by nuclear magnetic resonance (NMR) spectroscopy (see Table 1), with ¹¹⁹Sn being the preferred tin isotope as comparatively, it possesses the highest sensitivity. Solid-state NMR has indeed been applied to characterise structure and dynamics of α -SnF₂ [3–5]. However, mostly due to apparent inavailability of modern magic-angle spinning (MAS) equipment, the NMR data published so far neither achieve satisfactory site resolution for ¹⁹F [3, 4] nor for ¹¹⁹Sn [5].

Fig. 1

Table 1

Here we demonstrate that a reliable NMR characterization of tin(II) fluoride is feasible by using fast MAS and efficient ¹⁹F spin decoupling. The MAS spectra recorded under these conditions possess sufficient resolution to reveal the effects of indirect *J*-coupling. Unlike dipolar couplings, which act through space, *J*-couplings are mediated by covalent bonds, and are difficult to observe in solid-state NMR, because they are usually much smaller than dipolar couplings [6–8]. For ¹¹⁹Sn however, *J*-couplings tend to be comparatively large (in the range of kHz), and have been reported before in the literature for a variety of compounds [9–21]. The existence of *J*-couplings in α -SnF₂ shown here is further evidence for the existence of covalent Sn–F bonds in tin(II) fluoride.

2 Experimental

α -SnF₂ (99%) was purchased from Sigma Aldrich and used without further treatment. Phase purity was checked by powder XRD. Furthermore, the sample was inspected for elements other than Sn and F by EDX (energy-dispersive X-ray spectroscopy), but no evidence for such elements was found. Magic-angle spinning (MAS) ¹⁹F and ¹¹⁹Sn NMR spectra were recorded on a BRUKER DPX 400 spectrometer with a 9.4 T magnet, using a BRUKER MAS double-resonance probe with 2.5 mm rotors. The ¹⁹F spectrum at

60 kHz MAS was acquired on a BRUKER AVANCE III spectrometer equipped with a 14.1 T magnet, and a BRUKER MAS double-resonance probe with 1.3 mm rotors. Neither probe showed any substantial ^{19}F background signal. Recycle delays and number of transients are listed in the respective figure captions. For ^{19}F spin decoupling, the recently suggested $\text{SW}_f\text{-TPPM}$ sequence [22] was used. The sequence consisted of 11 pulse pairs with a phase angle of $\pm 12.5^\circ$, employing a linear sweep profile [23] with a sweep window from 0.69 – 1.46. These parameters were optimised on a fluorinated model compound. More details on the application of $\text{SW}_f\text{-TPPM}$ for ^{19}F decoupling will be published elsewhere [24]. The ^{19}F spectra were referenced against CFCl_3 by using solid CaF_2 as a secondary standard, with the ^{19}F resonance of CaF_2 assigned to -107.7 ppm [6]. Similarly, the ^{119}Sn NMR spectra were referenced by measuring SnO_2 as a secondary standard, setting this ^{119}Sn resonance at -604.3 ppm [25].

3 Results and Discussion

In comparison to NMR spectra recorded from solutions, static solid-state NMR spectra exhibit very broad, featureless resonances. For nuclei with spin $I = 1/2$, this is usually due to two predominant effects: (a) direct dipolar coupling (both homo- and heteronuclear), and (b) chemical shift anisotropy (CSA). Since both these effects have the same spatial dependence, they may be reduced or removed by application of magic-angle spinning (MAS) [6, 7]. The extent to which the broadening caused by dipolar couplings and CSA is removed from the spectrum depends on the relative magnitude of these interactions compared to the MAS frequency.

The magnitude of the dipolar interaction is determined by the angle θ_{jk} between the vector connecting the two spins j and k , and the direction of the external magnetic field, the gyromagnetic ratios γ_i of the involved nuclei, and the distance r_{jk} between the two spins [7]. The largest secular dipolar coupling, which is observed for $\theta_{jk} = 0$ (i.e. with the internuclear vector parallel to B_0) is usually called the *dipolar coupling constant*, b_{jk} . In units of Hertz, b_{jk} is given by Eq. 1.

$$b_{jk} = -\frac{\mu_0}{8\pi^2} \frac{\gamma_j \gamma_k \hbar}{r_{jk}^3} \quad (1)$$

1
2
3
4
5
6
7
8 The shortest distances for heteronuclear and homonuclear pairs of nuclei
9 reported for the X-ray structure [1] are 2.03 Å, namely between Sn(2) and
10 F(1), and 2.69 Å, between F(2) and F(4). With Eq. 1 and the γ_i values listed
11 in Table 1, we calculate maximum dipolar coupling constants of ≈ 5.0 kHz
12 for heteronuclear ^{119}Sn - ^{19}F couplings, and ≈ 5.5 kHz for homonuclear ^{19}F -
13 ^{19}F couplings. It has been estimated that MAS frequencies in excess of five
14 times the relevant dipolar interactions are necessary to completely remove
15 the dipolar broadening [6,26]. The second relevant interaction, the chemical
16 shift anisotropy (CSA), is also comparatively large for both ^{19}F and ^{119}Sn . In
17 the case of fluorine, CSA's of several hundred ppm's have been reported [27],
18 whereas for ^{119}Sn , CSA's up to a thousand ppm have been found [11]. For
19 a magnet with a field of 9.4 T, this translates into interactions between
20 40 kHz (^{19}F), and 150 kHz (^{119}Sn). Therefore, it is clear that very fast
21 MAS is needed to reduce both dipolar and CSA interactions sufficiently to
22 be able to resolve spectral lines belonging to different crystallographic sites
23 in α - SnF_2 .
24
25
26
27
28
29
30

31 As a third contribution to line broadening, J -couplings have to be taken
32 into account for ^{119}Sn , since it has been documented previously [9–21] that
33 they may also be of the order of kHz. In fact, the J -couplings for ^{119}Sn
34 can be so large that it has been possible to determine the anisotropy of
35 this interaction in some organo-tin compounds [14] by using off-magic angle
36 spinning. Under exact magic-angle spinning conditions, only the isotropic
37 part of the indirect J -coupling remains, but because of its comparatively
38 large magnitude, we expect J -couplings – if they are present – to affect the
39 NMR spectra of α - SnF_2 even at high MAS speeds.
40
41
42
43
44

45 3.1 ^{119}Sn MAS-NMR

46 In Fig. 2, the ^{119}Sn NMR spectra of α - SnF_2 at 25 kHz MAS are shown,
47 acquired with and without application of spin-decoupling on ^{19}F , under oth-
48 erwise identical conditions. It is obvious from Fig. 2b that residual dipolar
49 couplings (in combination with indirect J -couplings, see below) strongly
50 broaden the spectral lines, so application of efficient ^{19}F spin-decoupling is
51 essential. The sideband pattern observed in the ^{119}Sn NMR spectrum ac-
52 quired with decoupling (Fig. 2a) spans almost 1000 ppm, which is caused by
53 a large anisotropy of the chemical shift. Two isotropic bands (which do not
54
55
56
57
58
59
60

Fig. 2

1
2
3
4
5
6
7
8 alter position when the MAS speed is changed) are located at -949.4 and
9 -1024.7 ppm in the ^{119}Sn spectrum, which correspond to the two independ-
10 ent Sn positions in the crystal structure [1]. A better quality spectrum of
11 ^{119}Sn with ^{19}F spin-decoupling is shown in Fig. 3a. In this spectrum it can
12 be seen that the main lines of the sideband pattern are flanked by doublets
13 of satellite lines, with the spacing of these doublets being unaffected by the
14 spinning speed. These satellites should therefore be attributed to indirect
15 J -coupling between the magnetically active tin isotopes in $\alpha\text{-SnF}_2$. Because
16 of the very low natural abundance of ^{115}Sn , the presence of the satellite
17 lines is due mainly to coupling between the observed ^{119}Sn and neighbour-
18 ing $^{117,119}\text{Sn}$ isotopes. Since the natural abundance of both ^{117}Sn and ^{119}Sn
19 is below 9% (cf. Table 1), most of the observed ^{119}Sn nuclei are unaffected,
20 and only a small percentage contributes to the J -coupling satellites. To
21 determine the magnitude of the J -couplings, the high-intensity first-order
22 spinning sidebands were deconvoluted using the DMFIT program [28], as
23 shown in Fig. 3b. First, to ensure that the satellite doublet remains sym-
24 metric around the central line, the spinning sideband tool of DMFIT was used
25 to determine the positions of the satellites. These positions were then fixed,
26 and the intensity of the satellites was subsequently fitted with Lorentzian
27 lines, resulting in the deconvolution depicted in Fig. 3b. (The native J -
28 coupling tool in DMFIT could not be used because it expects both satellites
29 to have identical intensity, which our ^{119}Sn spectra do not always exhibit
30 because of the relatively poor signal-to-noise ratio.) The ^{119}Sn NMR spec-
31 trum of $\alpha\text{-SnF}_2$ can be fitted with a minimum of 3 doublets, resulting in
32 J -couplings of approximately 5.4, 3.3 and 1.4 kHz. We have also recorded
33 a Hahn-echo spectrum (not shown), where the observed satellite lines can
34 be caused by coupling of ^{119}Sn to ^{117}Sn only. Deconvolution of this echo
35 spectrum resulted in values very similar to those shown in Fig. 3b. However,
36 according to the connectivities that can be derived from the crystal struc-
37 ture of $\alpha\text{-SnF}_2$ [1,2], more than just the 3 satellites used for fitting here are
38 expected to show up in the spectrum. This will be discussed in more detail
39 below.

40
41
42
43
44
45
46
47
48
49
50
51
52
53
54
55
56 In terms of chemical bond character, it is instructive to compare the
57 findings presented here with a previous NMR study of SnO and SnO₂ [11].
58 Similar to $\alpha\text{-SnF}_2$, the ^{119}Sn spectrum of SnO displays a CSA-broadened
59
60

Fig. 3

1
2
3
4
5
6
7
8 spinning side band pattern spanning about 1000 ppm. This large anisotropy
9 in the shielding can be attributed to the presence of a stereochemically active
10 Sn lone electron pair in both compounds. Of course, such a lone pair is
11 absent in SnO₂, which is reflected in a comparatively small CSA of about
12 140 ppm [11]. Also, the tin spectra of SnO₂ do not exhibit any *J*-coupling
13 effects, since bonding is largely of ionic nature (rutile type). By contrast,
14 the significant degree of covalent character in SnO (PbO type) and α-SnF₂,
15 permits indirect spin coupling that is observed in the MAS spectrum of each
16 compound, with a *J* value of about 8 kHz in SnO [11]. Thus, the presence
17 of *J*-couplings in α-SnF₂ is additional evidence for the existence of genuine
18 covalent bonds, which has been deduced before from X-ray crystallography
19 by comparing the observed Sn–F distances to the sum of the respective ionic
20 radii [1].
21
22
23
24
25
26
27

28 3.2 ¹¹⁹Sn *J*-couplings and crystal structure

29
30 Since *J*-couplings are mediated by covalent bonds, the satellite pattern ob-
31 served in the ¹¹⁹Sn spectrum of α-SnF₂ (Fig. 3) should reflect the connectiv-
32 ities of the crystal structure, where the tin atoms are connected via fluorine
33 bridges. In general, a ¹¹⁹Sn NMR spectrum acquired with a single pulse
34 should show *J*-couplings for both ¹¹⁷Sn–F–¹¹⁹Sn and ¹¹⁹Sn–F–¹¹⁹Sn pairs,
35 whenever crystallographically distinct tin species are connected via Sn(1)–F–
36 Sn(2) bridges. For bridges among identical tin species, i.e. Sn(1)–F–Sn(1)
37 and Sn(2)–F–Sn(2), only ¹¹⁷Sn–F–¹¹⁹Sn couplings are relevant because of
38 the magnetic equivalence of crystallographically identical pairs. It also fol-
39 lows that bridges among identical species add to the *J*-coupling satellites
40 with only about half the intensity, because the ¹¹⁹Sn isotope does not con-
41 tribute.
42
43
44
45
46
47

48 However, the actual number of tin–fluorine–tin bridges existing in the
49 structure depends on which tin–fluorine distances are thought to represent
50 covalent bonds. When considering only distances up to the sum of the ionic
51 radii (2.27 Å according to Ref. [1]), the resulting structure consists of an
52 arrangement of Sn₄F₈ rings [1,2]. In this model, the two crystallographically
53 distinct tin species, designated Sn(1) and Sn(2), are connected via F(2)
54 and F(4) forming puckered rings. These rings possess comparatively short
55 bonds, from 2.068 to 2.273 Å. Clearly, the *J*-coupling observed in the ¹¹⁹Sn
56
57
58
59
60

spectrum is not consistent with having bonds only within these rings. If longer distances are also considered, additional bonds connect the Sn_4F_8 among themselves via fluorine bridges involving bond distances $> 2.4 \text{ \AA}$. This level of connectivity is used in the structural representation shown in Fig. 1. The co-ordination of this arrangement, as also described in Ref. [2], is such that the Sn(1) species are tetrahedrally surrounded by three fluorines and a lone pair, whereas Sn(2) is surrounded by five fluorine and a lone pair in octahedral fashion. Again, this structural model does not fit our ^{119}Sn NMR data, as it would result in different coupling patterns for the ^{119}Sn resonances belonging to Sn(1) and Sn(2), whereas we see a very similar satellite pattern for both. We may however find the desired equivalent co-ordination for both tin species if we include one further distance (2.675 \AA) as a bond into the model. As may be seen from Table 2, Sn(1) is now connected to four Sn(2) and two Sn(1) via various fluorine bridges. For Sn(2), the situation is identical in that it is connected to four Sn(1) and two Sn(2). With this model, we may explain the satellite pattern seen in the ^{119}Sn spectrum in the following way. The J -coupling via the shortest fluorine bridges (top two rows for each tin species in Table 2) is strongest, causing the satellites with about 5.4 kHz spacing. The remaining four fluorine bridges, involving at least one significantly longer tin–fluorine bond, all give rise to J -couplings of the order of 1.4 kHz, causing the inner satellites. As these are only visible as shoulders to the main line, fitting the exact positions is prone to some error. Since each tin species may experience the smaller J -coupling via four fluorine bridges, there is a reasonable probability that two magnetically active isotopes may be simultaneously present. This would result in a triplet structure caused by the J -coupling, and could explain the satellites with a spacing of about 3.3 kHz, if we accept that there is an error of about 0.2 kHz in the determination of the inner satellites. The 3.3 kHz satellites would thus represent the outer triplet lines (with corresponding low intensities), whereas the centre line of the triplet is hidden within the majority resonance of uncoupled nuclei.

With this model, we are able to qualitatively describe the appearance of the ^{119}Sn spectrum, however, the actual J -coupling pattern may be even more intricate. In particular, a roof effect could be expected for the ^{119}Sn – F – ^{119}Sn couplings, as the chemical shift difference between the two tin res-

Table 2

1
2
3
4
5
6
7
8 onances is only about 11 kHz at 9.4 T. Within the quality of the available
9 spectra, we do not observe such an effect, and other, unobserved subtleties
10 may be similarly present. Obviously, the resolution of the ^{119}Sn spectrum
11 would greatly benefit from faster MAS, but the 1.3 mm probe used for the
12 acquisition of the fast ^{19}F spectra at 60 kHz MAS does not reach the nec-
13 essary high resonance frequency for ^{119}Sn .
14

15
16
17 It should also be mentioned that the strongest J -coupling should exist
18 for the ^{19}F - ^{119}Sn pair, which is connected by a direct bond. Because ^{19}F
19 decoupling is applied, these couplings will be suppressed in the ^{119}Sn spec-
20 trum shown in Fig. 3. However, some evidence of tin-fluorine coupling can
21 be deduced from the ^{19}F MAS spectrum, as discussed below.
22
23
24

25 3.3 ^{19}F MAS-NMR

26
27 The ^{19}F NMR spectra of $\alpha\text{-SnF}_2$ at 25 kHz and 60 kHz MAS are shown
28 in Fig. 4. The spectrum at 25 kHz MAS (Fig. 4b) exhibits an extensive
29 sideband pattern, caused by a combination of residual dipolar couplings
30 and chemical shift anisotropy. At 60 kHz MAS (Fig. 4a), however, we can
31 expect the dipolar couplings to be completely averaged, so that the small
32 spinning sidebands still visible are caused by CSA only. Even at this high
33 spinning frequency, the two main ^{19}F bands remain fairly broad, with a
34 full-width-at-half-height (FWHH) of approximately 4 kHz. This broadening
35 must be attributed to a range of indirect J -couplings present in the bond
36 network of $\alpha\text{-SnF}_2$. Similar to the ^{119}Sn spectra discussed above, some
37 satellite lines can also be discerned in the ^{19}F spectra (indicated by arrows
38 in Fig. 4a). These satellites appear at a distance of approximately 8 and
39 4.5 kHz from the main band, are independent of the spinning speed, and
40 do not belong to 'probe background' (the latter was checked by measuring
41 other fluorinated compounds). The satellite line at 8 kHz (corresponding
42 to a J -coupling of 16 kHz) could tentatively be attributed to ^{19}F directly
43 bonded to ^{119}Sn , because of the strong coupling and the low intensity of the
44 satellite line. However, since the pairing lines of the satellite doublets are
45 hidden under the second main band, the analysis can not be conducted in
46 the same quantitative manner as for the ^{119}Sn spectra.
47
48
49
50
51
52
53
54
55

56 The considerable line broadening present in the ^{19}F NMR spectra of
57 $\alpha\text{-SnF}_2$, even at 60 kHz MAS, results in the observation of only two isotropic
58
59
60

Fig. 4

bands, which are centered around -42 and -50.5 ppm. Thus, the four fluorine sites reported in the crystal structure [1] cannot be fully resolved. In addition to the main bands, a low-intensity line is observed in the ^{19}F spectrum at around 113 ppm (marked by an asterisk in Fig. 4a), which remains narrow and stays at the same position also for lower spinning speeds. We attribute this line to some unknown minor impurity, which, judging from the small line width, appears to be very mobile. A chemically plausible candidate, which is also expected to show high mobility, would be hydrogen fluoride. Since the ^{19}F chemical shift of HF is known to depend very strongly on the environment [29], this is however difficult to verify.

4 Conclusions

Magic-angle spinning (MAS) NMR spectra of ^{19}F and ^{119}Sn have been recorded and analysed for the stable room-temperature phase of tin(II) fluoride, $\alpha\text{-SnF}_2$. The spinning sideband pattern observed for both nuclides indicate the existence of a large chemical shift anisotropy (CSA), which is consistent with the presence of a stereochemically active Sn lone electron pair. In the ^{119}Sn spectra, two isotropic bands are observed, belonging to the two independent Sn sites in the crystal structure [1]. Also, symmetric satellite lines with low intensity have been detected in the ^{119}Sn spectra, which are attributed to indirect J -couplings between the magnetically active tin isotopes. By spectral deconvolution of the satellite doublets, the J -couplings could be quantified to be 5.4, 3.3 and 1.4 kHz. By considering tin–fluorine distances of up to 2.675 Å to be covalent bonds, a structural model of $\alpha\text{-SnF}_2$ could be found that qualitatively explains the observed J -coupling pattern. Indications for the presence of J -couplings have also been found in the ^{19}F spectrum of $\alpha\text{-SnF}_2$. Quite uncommonly, J -coupling thus appears to be the main source of the considerable ^{19}F line broadening still present in the 60 kHz MAS spectrum. This residual line broadening does not permit sufficient resolution to observe all four fluorine sites reported in the crystal structure [1]. The detection of J -couplings is in itself evidence for the existence of genuine covalent bonds in $\alpha\text{-SnF}_2$, a fact which has been deduced before from X-ray crystallography by identifying Sn–F distances smaller than the sum of the respective ionic radii [1].

5 Acknowledgments

We would like to thank C. Vinod Chandran and Ivan Halasz (MPI Stuttgart) for skillful help in preparing the figures for this article. Sharon Ashbrook, John Griffin and Phil Wormald (St. Andrews, UK) are acknowledged for their instrumental assistance to acquire the ^{19}F -MAS spectrum at 60 kHz.

References

- [1] R.C. McDonald, H. Ho-Kuen Hau, K. Eriks, *Inorg. Chem.* **1976**, *15*, 762.
- [2] G. Denes, J. Pannetier, J. Lucas, J. Y. Le Marouille, *J. Solid State Chem.* **1979**, *30*, 335.
- [3] J. Pannetier, G. Denes, M. Durand, J.L. Buevoz, *J. Physique* **1980**, *41*, 1019.
- [4] A. T. Kreinbrink, C.D. Sazavsky, J. W. Pyrz, D.G.A. Nelson, R.S. Honkonen, *J. Magn. Reson.* **1990**, *88*, 267.
- [5] G. Neue, S. Bai, R.E. Taylor, P.A. Beckmann, A.J. Vega, C. Dybowski, *Phys. Rev. B* **2009**, *79*, 214302.
- [6] R.K. Harris, P. Jackson, *Chem. Rev.* **1991**, *91*, 1427.
- [7] M.H. Levitt, *Spin Dynamics: Basics of Nuclear Magnetic Resonance*, Wiley & Sons, Chichester **2008**.
- [8] D. Massiot, F. Fayon, M. Deschamps, S. Cadars, P. Florian, V. Montouillot, N. Pellerin, J. Hiet, A. Rakhmatullin, C. Bessada, *C. R. Chimie* **2010**, *13*, 117.
- [9] R.K. Harris, A. Sebald, *Magn. Reson. Chem.* **1987**, *25*, 1058.
- [10] A. Lyčka, J. Holeček, B. Schneider, J. Straka, *J. Organomet. Chem.* **1990**, *389*, 29.
- [11] C. Cossement, J. Darville, J.-M. Gilles, J. B. Nagy, C. Fernandez, J.-P. Amoureux, *Magn. Reson. Chem.* **1992**, *30*, 263.

- 1
2
3
4
5
6
7
8 [12] C. Mundus, G. Taillades, A. Pradel, M. Ribes, *Solid State Nucl. Magn. Reson.* **1996**, 7, 141.
9
10
11 [13] J.C. Cherryman, R.K. Harris, *J. Magn. Reson.* **1997**, 128, 21.
12
13 [14] C. Marichal, A. Sebald, *Chem. Phys. Lett.* **1998**, 286, 298.
14
15 [15] H. Lock, J. Xiong, Y.-C. Wen, B.A. Parkinson, G.E. Maciel, *Solid State Nucl. Magn. Reson.* **2001**, 20, 118.
16
17 [16] M. Bechmann, X. Helluy, C. Marichal, A. Sebald, *Solid State Nucl. Magn. Reson.* **2002**, 21, 71.
18
19 [17] C. Camacho-Camacho, R. Contreras, H. Nöth, M. Bechmann, A. Sebald, W. Milius, B. Wrackmeyer, *Magn. Reson. Chem.* **2002**, 40, 31.
20
21 [18] S.P. Gabuda, V.Y. Kavun, S.G. Kozlova, V.V. Tverskikh, *Russ. J. Coord. Chem.* **2003**, 29, 1.
22
23 [19] P. Amornsakchai, D.C. Apperley, R.K. Harris, P. Hodgkinson, P.C. Waterfield, *Solid State Nucl. Magn. Reson.* **2004**, 26, 160.
24
25 [20] J. Beckmann, D. Dakternieks, A. Duthie, *Organometallics* **2005**, 24, 773.
26
27 [21] A. Bagno, G. Casella, G. Saielli, *J. Chem. Theory Comput.* **2006**, 2, 37.
28
29 [22] R. S. Thakur, N. D. Kurur, P. K. Madhu, *Chem. Phys. Lett.* **2006**, 426, 459.
30
31 [23] C. V. Chandran, P.K. Madhu, N. D. Kurur, T. Bräuniger, *Magn. Reson. Chem.* **2008**, 46, 943.
32
33 [24] C. V. Chandran, P. K. Madhu, P. Wormald, T. Bräuniger, *submitted* **2010**
34
35 [25] S. Chaudhuri, F. Wang, C.P. Grey, *J. Am. Chem. Soc.* **2002**, 124, 11746.
36
37 [26] E. Brunner, D. Fenzke, D. Freude, H. Pfeifer, *Chem. Phys. Lett.* **1990**, 169, 591.
38
39
40
41
42
43
44
45
46
47
48
49
50
51
52
53
54
55
56
57
58
59
60

- 1
2
3
4
5
6
7
8 [27] M. Mehring, *High Resolution NMR Spectroscopy in Solids*, Springer,
9 Berlin/Heidelberg/New York, **1983**, Chapter 7.4.
10
11 [28] D. Massiot, F. Fayon, M. Capron, I. King, S. Le Calve, B. Alonso, J.
12 Durand, B. Bujoli, Z. Gan, G. Hoatson, *Magn. Reson. Chem.* **2002**,
13 *40*, 70.
14
15 [29] J.-C. Culmann, M. Fauconet, R. Jost, J. Sommer, *New. J. Chem.* **1999**,
16 *23*, 863.
17
18 [30] R.K. Harris, E.D. Becker, S.M. Cabral de Menezes, R. Goodfellow, P.
19 Granger, *Concepts Magn. Reson.* **2002**, *14*, 326.
20
21
22
23
24
25
26
27
28
29
30
31
32
33
34
35
36
37
38
39
40
41
42
43
44
45
46
47
48
49
50
51
52
53
54
55
56
57
58
59
60

Table 1. Nuclear properties of the NMR-observable nuclei in SnF₂ (from Ref. [30]).

Isotope	Spin I	Natural abundance	Magnetogyric ratio, γ ^a	Relative receptivity ^b	Frequency ratio ^c
¹⁹ F	$\frac{1}{2}$	100%	25.181	0.834	94.094 MHz
¹¹⁵ Sn	$\frac{1}{2}$	0.34%	-8.801	1.21×10^{-4}	32.718 MHz
¹¹⁷ Sn	$\frac{1}{2}$	7.68%	-9.588	3.54×10^{-3}	35.632 MHz
¹¹⁹ Sn	$\frac{1}{2}$	8.59%	-10.032	4.53×10^{-3}	37.290 MHz

^a in 10^7 rad s⁻¹ T⁻¹

^b Receptivity relative to ¹H.

^c With ¹H at 100 MHz.

Table 2. Distances within tin–fluorine–tin bridges in α -SnF₂, calculated from the co-ordinates published in Ref. [1].

Sn(1) –	2.098 Å	– F(2) –	2.204 Å	– Sn(2)
	2.148 Å	– F(4) –	2.273 Å	– Sn(2)
	2.068 Å	– F(3) –	2.474 Å	– Sn(2)
			2.675 Å	– Sn(1)
	2.675 Å	– F(3) –	2.474 Å	– Sn(2)
			2.068 Å	– Sn(1)
Sn(2) –	2.204 Å	– F(2) –	2.098 Å	– Sn(1)
	2.273 Å	– F(4) –	2.148 Å	– Sn(1)
	2.474 Å	– F(3) –	2.068 Å	– Sn(1)
			2.675 Å	– Sn(1)
	2.027 Å	– F(1) –	2.401 Å	– Sn(2)
	2.401 Å	– F(1) –	2.027 Å	– Sn(2)

Figure Captions

Figure 1: The structure of the monoclinic phase of tin(II) fluoride, α -SnF₂, based on the co-ordinates published in Ref. [1]. Puckered rings with comparatively short bonds are formed by tin (Sn(1) and Sn(2), dark spheres) and fluorine (F(2) and F(4), light spheres), which are emphasized in the drawing. These rings are connected via the F(1) species along the *a*-axis direction, and via F(3) along the *c*-axis direction [1, 2], involving longer bond distances ($> 2.4 \text{ \AA}$).

Figure 2: ¹¹⁹Sn MAS NMR spectra at 25 kHz spinning speed (2k accumulations, 25 s recycle delay): (a) with, and (b) without ¹⁹F spin decoupling. The isotropic bands (marked by arrows) are located at -949.4 and -1024.7 ppm, respectively.

Figure 3: ¹¹⁹Sn MAS NMR spectrum at 25 kHz spinning speed (5k accumulations, 60 s recycle delay): (a) full MAS spectrum, (b) deconvolution of satellites caused by *J*-coupling, using the high-intensity first-order spinning sidebands, which are marked by arrows in (a). The spectrum can be fitted with a minimum of 3 doublets, with *J*-couplings of approximately 5.4, 3.3 and 1.4 kHz. From structural data [1, 2], however, an entire range of *J*-couplings is expected, which are not resolved here.

Figure 4: ¹⁹F MAS NMR spectra: (a) 60 kHz spinning speed (32 accumulations, 5 s recycle delay); (b) 25 kHz spinning speed (128 accumulations, 10 s recycle delay). The isotropic bands are centered around -42 and -50.5 ppm, respectively. The arrows in (a) indicate satellite lines attributed to *J*-couplings, whereas the asterisk marks a line due to an impurity (see text for details).

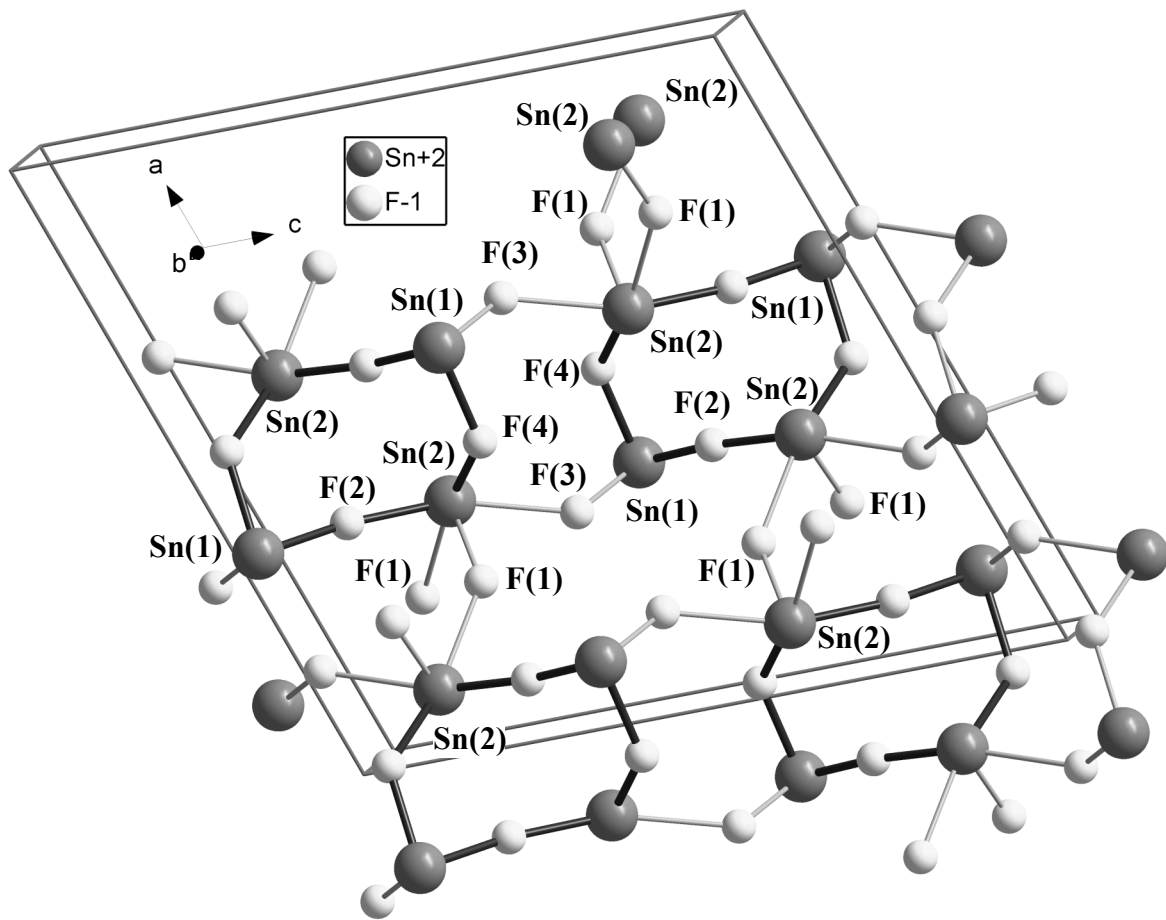
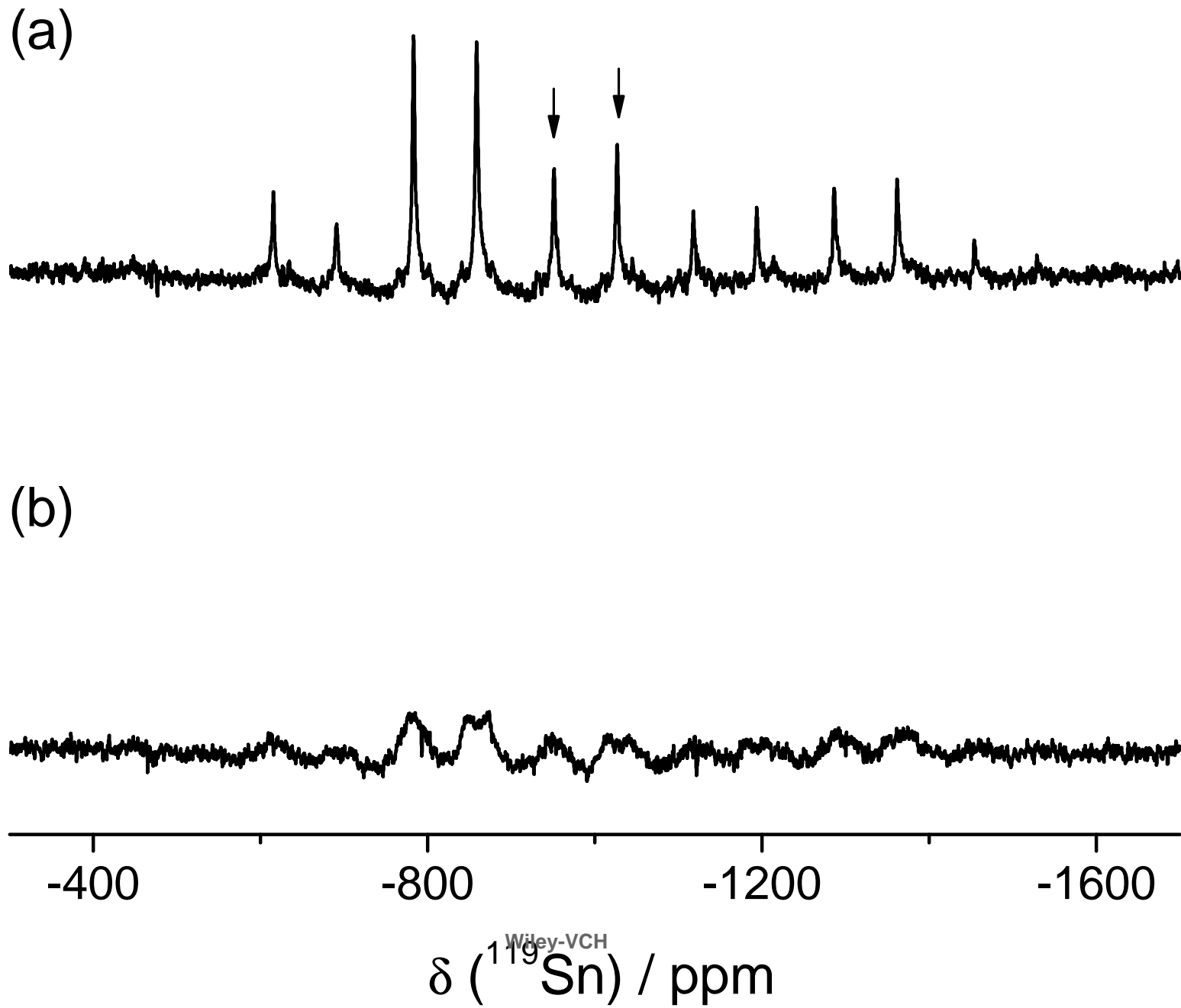
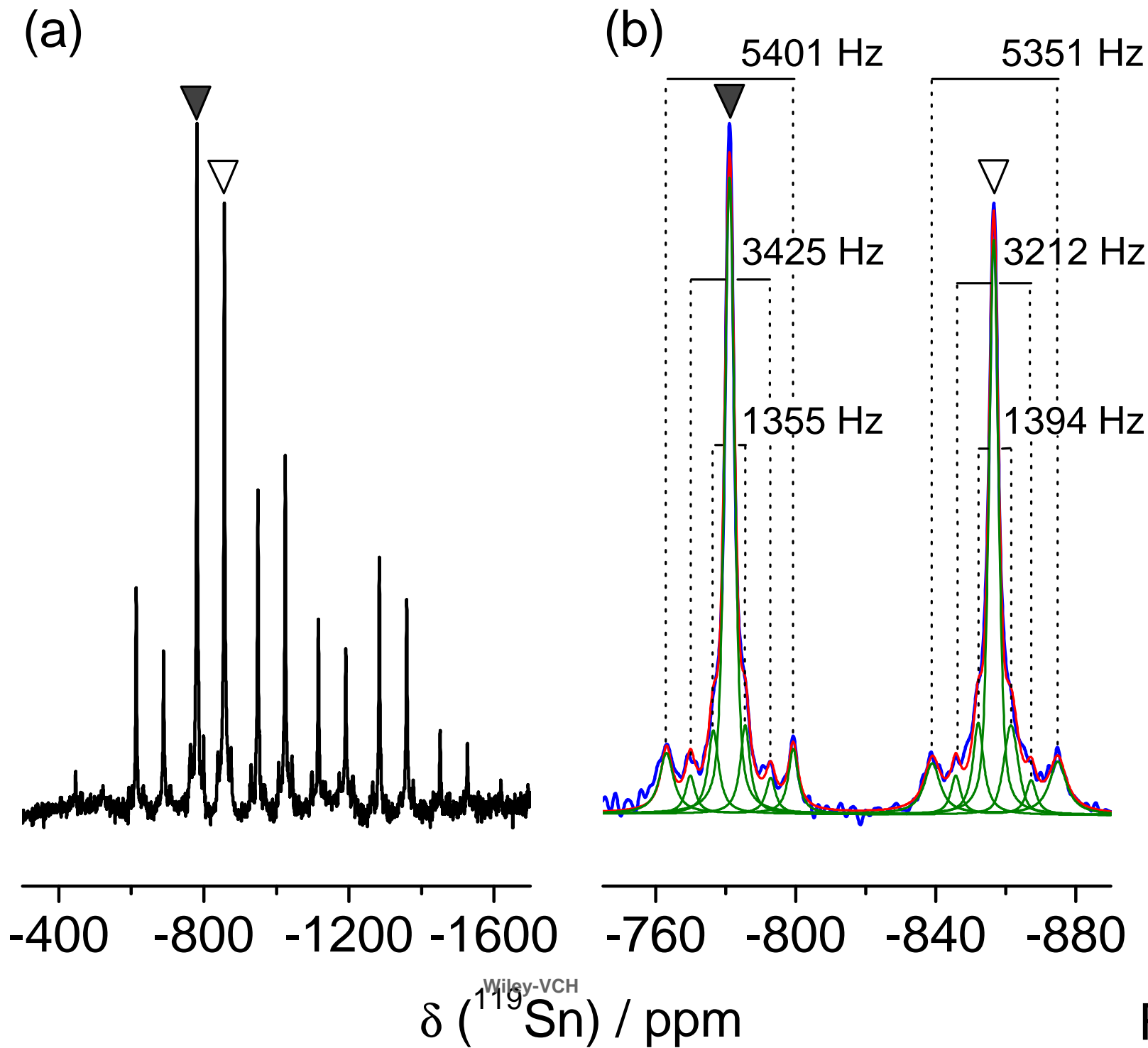


Fig. 1





ZAAC

MAS

(a)

60 kHz

(b)

25 kHz

100

0

-100

-200

$\delta (^{19}\text{F}) / \text{ppm}$

Fig.4

